GEOPHYSICAL RESEARCH LETTERS, VOL. 36, L14607, doi:10.1029/2009GL038569, 2009

Vertical motion in the upper ocean from glider and altimetry data

Simón Ruiz,[1] Ananda Pascual,[1] Bartolomé Garau,[1] Isabelle Pujol,[2] and Joaquín Tintoré[1]

Received 7 April 2009; revised 29 May 2009; accepted 16 June 2009; published 23 July 2009.

[1] This study represents a first attempt to combine new glider technology data with altimetry measurements to understand the upper ocean dynamics and vertical exchanges in areas with intense horizontal density gradients. In July 2008, just two weeks after Jason-2 altimeter was launched, a glider mission took place along a satellite track in the Alboran Sea (Western Mediterranean). The mission was designed to be almost simultaneous with the satellite passage. Dynamic height from glider reveals a sharp gradient (~15 cm) and corresponds very well with the absolute dynamic topography from Jason-1 & Jason-2 tandem mission ($r > 0.97$, rms differences < 1.6 cm). We blend both data sets (glider and altimetry) to obtain a consistent and reliable 3D dynamic height field. Using quasi-geostrophic dynamics, we diagnose large-scale vertical motions (~1 m day^{-1}) which may provide a local mechanism for the subduction of the chlorophyll tongue observed by the glider. **Citation:** Ruiz, S., A. Pascual, B. Garau, I. Pujol, and J. Tintoré (2009), Vertical motion in the upper ocean from glider and altimetry data, *Geophys. Res. Lett.*, *36*, L14607, doi:10.1029/2009GL038569.

1. Introduction

[2] Improving our knowledge on the relationship between the physical and biological processes in the upper ocean is essential for understanding and predicting how the ocean and the marine ecosystems respond to changes in the climate system. Vertical motion associated with mesoscale oceanic features such as fronts, meanders, eddies and filaments is of fundamental importance for the exchanges of heat, fresh water and biogeochemical tracers between the surface and the ocean interior [*Siedler et al.*, 2001]. In particular, the sinking of organic matter represents a key mechanism (biological pump) to transport CO_2 from surface to deep ocean layer [*McGillicuddy et al.*, 2007]. Unfortunately, it is not yet possible to make direct measurements of vertical velocities less than 1000 m day^{-1} [*Allen et al.*, 2001a]. Instead, it can be inferred from a 3D snapshot of the density field by assuming a few simplifications in the quasi-geostrophic (QG) formulation [*Hoskins et al.*, 1978]. The use of this approximation has allowed the understanding of the structure and dynamics of mesoscale structures in the upper ocean [*Dewey et al.*, 1991; *Lindstrom and Watts*, 1994; *Gomis et al.*, 2001], as well as proposing empirical models that relate the magnitude of vertical motion to the slope of the size (abundance spectrum) of phytoplankton in a frontal ecosystem [*Rodríguez et al.*, 2001].

[3] In this context, we investigate the feasibility of diagnosing vertical velocity combining gliders and satellite data. Gliders are autonomous underwater vehicles providing high resolution hydrography and biogeochemical data of the ocean. These platforms have recently been used to monitor the coastal variability in the Western Mediterranean and have shown the potential benefit when they are combined with altimetry [*Ruiz et al.*, 2009]. In a first step, we use an Empirical Orthogonal Function (EOF) decomposition to merge one transect of high resolution hydrographic glider data and altimetry gridded fields, inferring the 3D density field in the Eastern Alboran Sea (Western Mediterranean). In this area, the jet of Atlantic Water forms the head of the so-called Algerian Current that flows along the African continental slope [*Millot*, 1985]. This transition zone between the Alboran Sea and the Algerian Sub-basin is one of the less known current systems in the western Mediterranean. In a second step, we use the QG Omega equation to examine vertical velocity and its consistence with biological measurements from glider. Furthermore, the data set presented in this work represent an unique opportunity for comparison between high resolution in-situ records and the first data provided by the Jason-2 new altimeter mission.

2. Data and Methods

2.1. Glider Data

[4] For this experiment, we used a Slocum coastal glider that collected 1311 profiles (CTD, fluorescence and turbidity) between the surface and 180 m. The mission took place from July 4 to 18, 2008 and was designed to cross the Eastern Alboran Sea, from approximately 30 miles east of the Spanish coast of Cartagena and towards 20 miles off the Algerian coast (Figure 1a). The along-track glider data resolution is about 0.5 km. All variables gathered have been averaged vertically to 1 dbar bins. The glider trajectory was established to be coincident with the altimetry satellite track 172 of the tandem mission Jason-1 and Jason-2.

2.2. Altimetry Data

[5] Jason-2 was launched on June 20, 2008 and the first measurements were available on July 4, once the new satellite reached its operational orbit of 1,336 kilometres. During Jason-2 calibration phase, both satellites were flying in formation in the same orbit approximately 55 seconds apart. In this study we use the along-track data from both altimeters provided by AVISO. The processing follows the standard approach. The sea surface height is corrected for geophysical effects and resampled every 7 km. Sea level anomalies are obtained by removing a 7-year mean and a low-pass filtered is applied to reduce measurement noise [*Dibarboure et al.*, 2008]. Absolute dynamic topography is computed by adding a mean dynamic topography [*Rio et*

[1]Instituto Mediterraneo de Estudios Avanzados, IMEDEA (CSIC-UIB), Esporles, Spain.
[2]CLS, Ramonville Saint-Agne, France.

0094-8276/09/2009GL038569$05.00

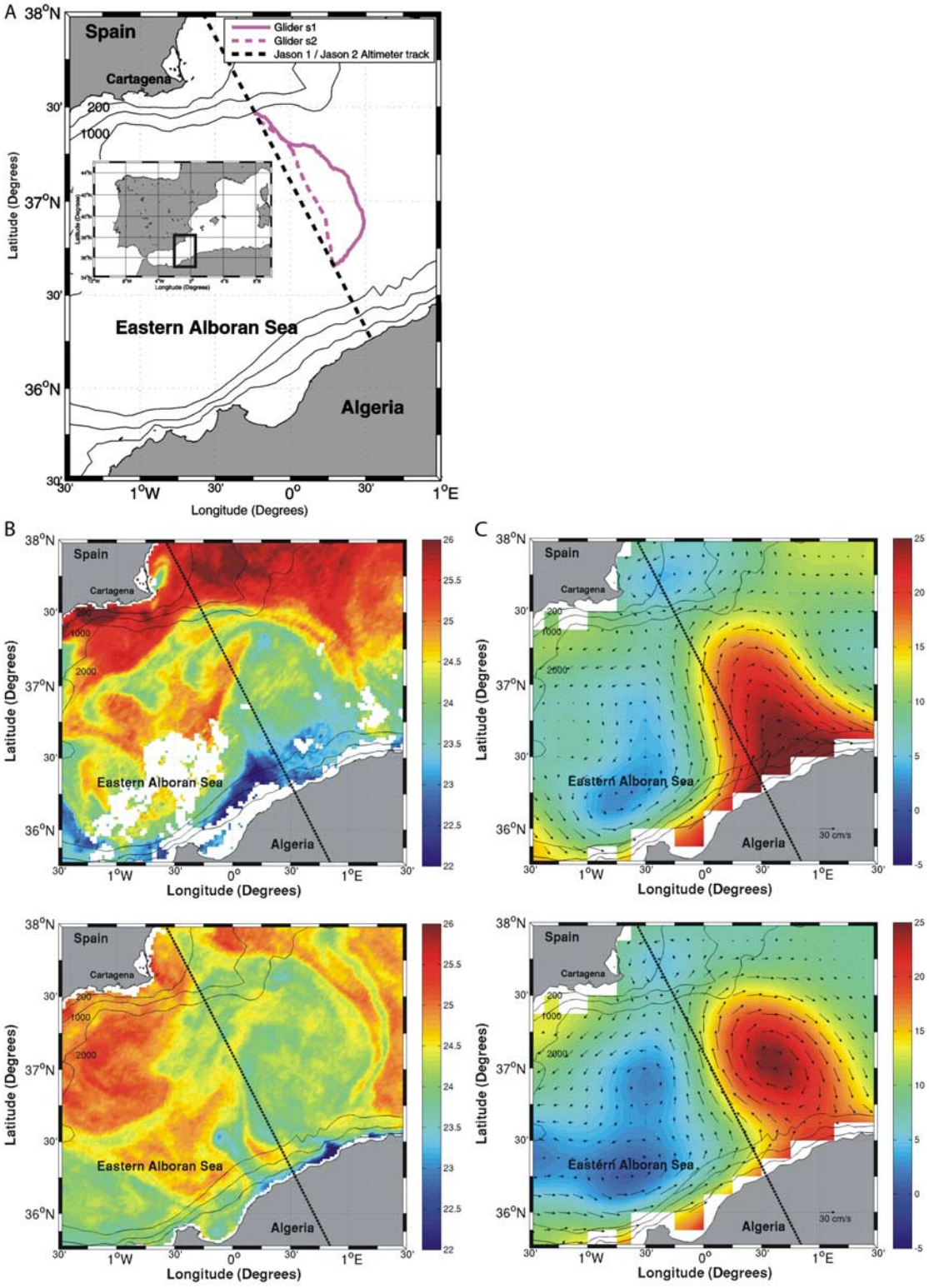

Figure 1. (a) Study area showing the gliders tracks (solid and dashed magenta lines) during the Alboran 2008 mission and 172 Jason-1/Jason-2 altimeter track (dashed black line), (b) night AVHRR SST images for 7 and 23 July 2008. The temperature scale is in °C. Details about the algorithms and processing methods applied to the images can be found in O&SI SAF project team (2005), (c) interpolated altimeter maps of ADT for same date with surface geostrophic currents overimposed.

al., 2007] to the sea level anomalies. In addition, we use the interpolated real-time gridded fields which combine Jason-1 and ENVISAT along-track measurements (Jason-2 is not included in the gridded products during the calibration period). AVISO provides specific maps for the Mediterranean Sea, which are computed on a regular 1/8° grid applying a suboptimal space/time objective analysis [*Le Traon and Ogor*, 1998]. This analysis is performed using space and time correlation functions with zero-crossing points at 100-km and 10 days, respectively. Note that through this interpolation analysis, the scales that cannot be properly resolved by the altimeter data are filtered out (meso and sub-mesoscale) and consequently the magnitude of high-derivatives variables computed is significantly reduced [*Gomis et al.*, 2001].

2.3. Three-Dimensional Reconstruction of *dh* Field

[6] The EOF decomposition of dynamic height (DH) provides the dominant modes (vertical-dependent) and amplitudes (horizontal dependent) along the glider track. To obtain a 3D field, *Pascual and Gomis* [2003] developed and tested a method that combines these vertical modes and the gridded altimetry data to infer the vertical structure of DH field. The method is based on the assumption that altimetry provides a reliable measure of DH and that the glider profiles are enough as to compute statistically significant EOFs. Alternatively, the modes can be computed from historical data (CTDs, XBTs, Niskin bottles) as it was done by *Pascual and Gomis* [2003], or even from ARGO floats. In our case, the glider platform provides a high number of observations (more than 1300 hydrographic profiles) that are consistent in terms of data processing. Moreover, these hydrographic data (and derived variables) allow a direct and unique comparison to altimeter Jason-1 and Jason-2 measurements.

[7] In the case of a single dominant mode, the modelled profile can be expressed as:

$$\Phi_{x,y}(p) = A_1(x,y)EOF_1(p). \quad (1)$$

Thus, obtaining the single amplitude corresponding to each profile $A_1(x, y)$ would be straightforward given the surface altimetry data $[\Phi_{x,y}(p_0)]$ and the surface component of the leading EOF $[EOF_1(p_0)]$ from glider data.

2.4. Computation of Vertical Velocities

[8] To quantify the vertical motion, we use the diagnostic QG omega equation, which is directly obtained from the QG vorticity and thermodynamic equation [*Hoskins et al.*, 1978]:

$$f^2\frac{\partial^2\omega}{\partial z^2} + \left(\frac{\partial^2}{\partial x^2} + \frac{\partial^2}{\partial y^2}\right)(N^2\omega) = \nabla_h Q \quad (2)$$

where $Q = \left[2f\left(\frac{\partial V}{\partial x}\frac{\partial U}{\partial z} + \frac{\partial V}{\partial y}\frac{\partial V}{\partial z}\right), -2f\left(\frac{\partial U}{\partial x}\frac{\partial U}{\partial z} + \frac{\partial U}{\partial y}\frac{\partial V}{\partial z}\right)\right]$ and (U, V) are the geostrophic velocity components. By assuming a boundary conditions for ω and from a 3D snapshot of the density field, the vertical velocity can be inferred. We set $w = 0$ at the upper and lower boundaries and Neumann conditions at the lateral boundaries (see *Pinot et al.* [1996] for a detailed description of the method). The extension of the domain over which ω is calculated has been limited to the area (and nearby area) covered by observations. This ensures a correct representativity of the vertical modes used to reconstruct the 3D dh field.

3. Results and Discussion

3.1. Synoptic View From Remote Sensing Data

[9] Sea Surface Temperature (SST) and interpolated altimetry maps provide a synoptic view of the mesoscale and large-scale activity at the study area during the glider mission (Figure 1b). At the beginning of July, SST images reveal the presence of a relative cold jet flowing along the African coast (Atlantic jet) and a mesoscale instability developing between 0° and 0.5°E (beginning of the Algerian Current). After 2 weeks, this instability becomes an antyciclonic eddy of about 90 km diameter with a clear eastward displacement and secondary filaments interacting with warmer Mediterranean Water in the edge of the eddy. Altimetry maps, with associated horizontal geostrophic velocities of about 50 cms^{-1} (Figure 1c), confirm the evolution of these structures.

3.2. Glider Vertical Sections

[10] Below the surface, the very high-resolution in-situ data from glider shows the existence of strong interleaving features (Figure 2). In the northern part, characterized by strong surface density gradients of about 1.5 sigma-t difference in about 20 km, fluorescence data suggest the existence of significant downward motion with important bio-geochemical implications, in agreement with original observations in the area [*Tintoré et al.*, 1988]. Chlorophyll subsurface maxima are clearly observed along the section and there is evidence, close to the front, of phytoplankton extending in a tongue down to near 180 meters. This tongue coincides with the frontal zone defined by the temperature and salinity data from glider (Figure 2) and suggests the subduction of water from the dense side of the front, below the frontal structure. At surface (~20m), we found the lowest salinity waters of Atlantic origin with values of about 36.3 PSU, that are referred to as recent Atlantic Water (AW) [*Arnone et al.*, 1990]. The subducted water corresponds to Mediterranean Surface Water (MSW) (Salinity > 37.5, temperature > 15.5°C) whose origin is mainly old AW remained at surface in the Western Mediterranean [*Benzohra and Millot*, 1995]. This water flows southwestward along the Spanish coast producing a frontal area with the recent AW from the Strait of Gibraltar.

3.3. Three-Dimensional Dynamic Height

[11] As reference level for DH computation, we choose the deepest level (180 m) from glider. Previous authors [*Tintoré et al.*, 1988] have considered levels of no motion at around 200 m and *Allen et al.* [2001a] confirmed this view with observations from an intense sampling with SeaSoar and ADCP. Direct estimations of DH from glider profiles reveal the sharp gradient (~15 cm) and corresponds very well with the absolute dynamic topography (ADT) [*Rio et al.*, 2007] obtained from Jason-1 and Jason-2 tandem mission (Figure 3a). The correlation (RMS) between the ADT from Jason-1 and Jason-2 and DH from glider is 0.97 (1.4 cm) and 0.99 (1.6 cm), respectively. This remarkable

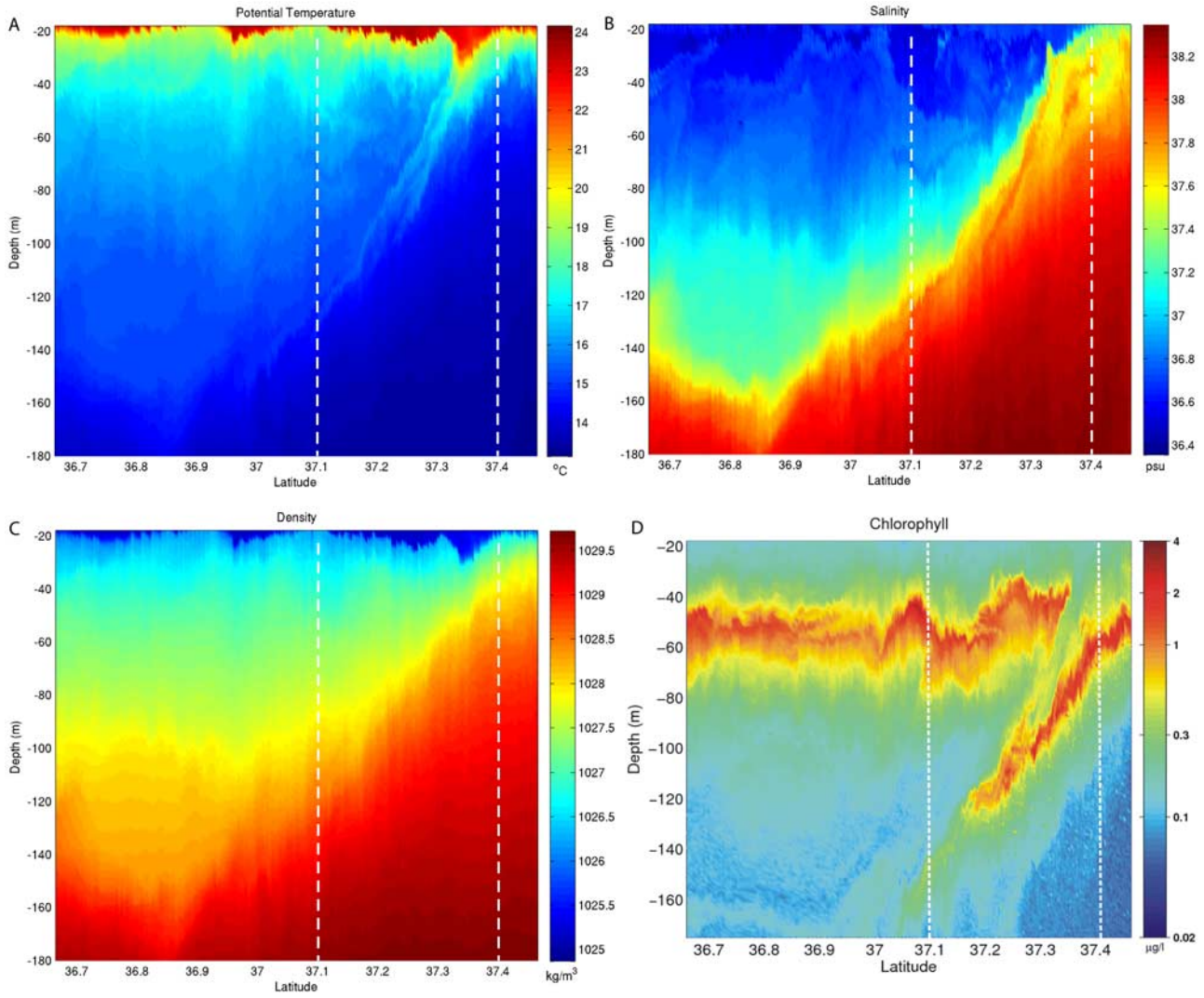

Figure 2. Vertical section of temperature (°C), salinity (PSU), density (kg/m^3) and chlorophyll (μg/l) from glider section 2 (dashed magenta in Figure 1). White dashed lines define sub-section in the northern part of the domain.

good agreement, together with the fact that the first DH vertical mode accounts for 98.4% of the total variance (see auxiliary material), justifies the application of equation (1).[1] This result is in agreement with the value reported in the same area by *Pascual* [2003], who found that the first mode accounted for 98% of the variance. In other areas, such as the Balearic Sea, where dynamics is different, the percentage accounted by the first mode is reduced to 80% [*Pascual and Gomis*, 2003]. The standard deviation between original glider and reconstructed DH profiles is 0.64 cm, which represents an error variance (relative to the original DH variance) of 3%. For density, the standard deviation of the differences and the error variance are 0.17 kg/m^3 and 4%, respectively (see auxiliary material). These low error values prove that the reconstruction technique performs extremely well. The reconstructed DH field (Figure 3b) reveals the presence of an intense antyclonic eddy with a southeast-northwest gradient of about 10 cm at 75 m and maximum velocities associated of 35 cms^{-1}. The partial view of the structure showed in Figure 3b is in agreement with the description given in the previous section.

3.4. Vertical Velocities

[12] Figure 3c shows the QG vertical velocities derived from the reconstructed DH field. The pattern is characterized by downward (upward) motion in the northern (southern) part of the domain, downstream (upstream) of the gyre with maximum values of about ±1 m day^{-1} at 75 m depth. These diagnosed vertical velocities are smaller than expected according to the density gradients observed in the in-situ data. However, as it was stressed in previous studies [*Tintoré et al.*, 1991; *Pollard and Regier*, 1992; *Gomis and Pedder*, 2005], the magnitude of the vertical velocity is significantly sensitive to the scales included in the analysis. Although the gridded altimeter maps resolution 1/8° (∼11 km) used in this study is smaller than the typical Rossby radius in the area (20 km [*Tintoré et al.*, 1991]), we

[1]Auxiliary materials are available in the HTML. doi:10.1029/2009GL038569.

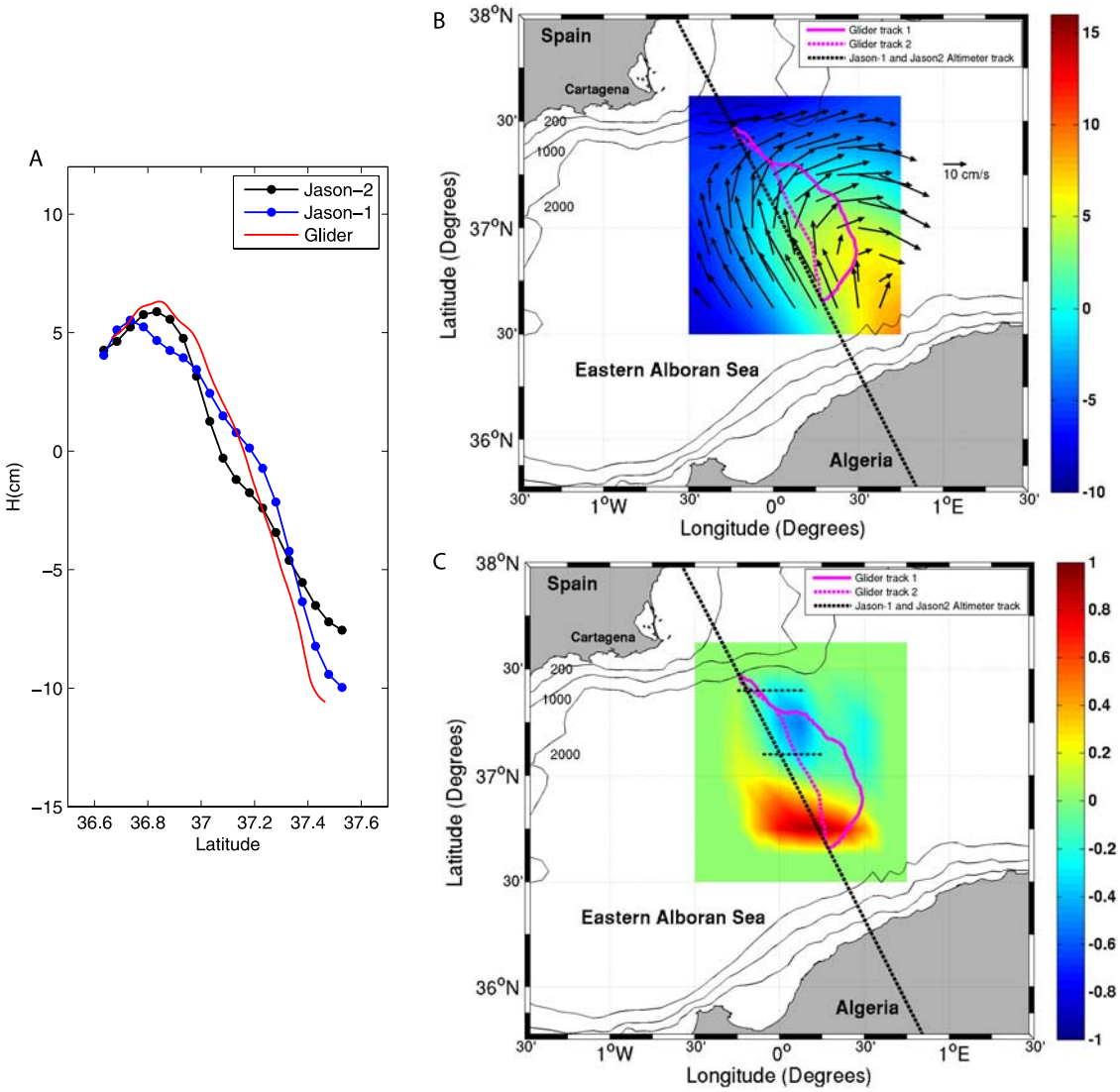

Figure 3. (a) Dynamic height computed along glider track and Absolute Dynamic Topography along 172 Jason-1 and Jason-2 altimeters track. Units are cm. (b) Reconstructed dynamic height (cm) and geostrophic velocity (cms^{-1}) at 75 m. (c) Quasi-Geostrophic vertical velocity at 75 m. Units are m day^{-1}, positive/negative values indicate upward/downward motion. The latitude limits of sub-section defined in Figure 2 are here indicated as black dot-dashed line.

recall that the smaller resolvable scale by the altimeter data is ∼100 km.

4. Conclusions

[13] This study represents a first attempt on the combination of new glider technology data with altimetry observations to diagnose vertical velocities. First, we have shown that the high resolution DH derived from the new autonomous vehicle and the ADT from Jason-1 and Jason-2 tandem mission reveals high correlations along the track followed by the three platforms. Based on these correlations, our method blends along-track glider data with gridded altimeter fields to provide a consistent and reliable 3D DH field. With the reconstructed field and using the QG theory, results show that Mediterranean Surface Water (MSW) is advected westwards along the Spanish coast subducting in the frontal region below the recent Atlantic Waters at an estimated rate of -1 m day^{-1}. The vertical motion diagnosed in our work is consistent (although the magnitude is smaller) with previous observational [*Allen et al.*, 2001a; *Shearman et al.*, 1999] and modeling [*Strass*, 1994; *Allen et al.*, 2001b] studies in adjacent areas and may provide a local mechanism for the subduction of the chlorophyll tongue observed by the glider. Note that the vertical motion reported in this work is associated with the large-scale field observed in the study area. *Tintoré et al.* [1991] also found vertical velocities of ±1 $mday^{-1}$ associated with the large scale circulation (∼90 km diameter eddies observed in the Alboran Sea) and 20–25 $mday^{-1}$ related to the meso and submesoscale circulation. Thus, in the present work, we find coherent values of vertical velocities (±1 $mday^{-1}$) associated with the large scales resolved by altimetry (diameter ∼100 km).

[14] This work has demonstrated the mature state of the altimetry providing high quality and reliable data just 2 weeks after Jason-2 mission was launched. Moreover, we have shown the potential benefit of combining the

altimetry monitoring with in-situ data from autonomous underwater vehicles for a better understanding of the dynamics in the upper ocean. The major limitation of the proposed method comes from the horizontal scales resolved by the altimeter gridded fields. By increasing the number of altimeters merged in the analysis (see, for instance, *Pascual et al.* [2006]), the mesoscale activity is better described, smaller features can be resolved and more accurate values of vertical velocities could be estimated. In the longer term, high-spatial resolution of the ocean surface topography will be available thanks to the SWOT mission and the proposed method could be improved and would provide a better characterization of the vertical motions associated with eddy fields in the open ocean and coastal regions. Alternative ways to proceed would be to use SST measurements from high resolution infrared images to complement altimeter data as it has been shown by *LaCasce and Mahadevan* [2006].

[15] **Acknowledgments.** The altimeter data were produced by SSALTO/DUACS and distributed by AVISO with support from CNES. Special thanks to B. Casas, M. Martínez-Ledesma and M. Bonet for their efficient collaboration during the glider mission. First author thanks J. Wilkin and D.P. Wang for their comments during the initial phase of this work. The overall framework of this work is the EU-funded SESAME project (contract GOCE-2006-036949). Partial support from COOL project (contract CTM2006-12072/MAR) funded by the Spanish Marine Science and Technology program is also acknowledged. Finally, we would like to extend our acknowledgment to the Fuerza de Acción Marítima (FAM) from the Spanish Navy.

References

Allen, J. T., D. A. Smeed, J. Tintoré, and S. Ruiz (2001a), Mesoscale subduction at the Almeria-Oran front. Part 1: Agesotrophic flow, *J. Mar. Syst.*, *30*, 263–285, doi:10.1016/S0924-7963(01)00062-8.

Allen, J. T., D. A. Smeed, A. J. G. Nurser, J. W. Zhang, and M. Rixen (2001b), Diagnosing vertical velocities with the QG omega equation: an examination of the errors due to sampling strategy, *Deep Sea Res., Part I*, *48*, 315–346, doi:10.1016/S0967-0637(00)00035-2.

Arnone, R. A., D. A. Wiesenburg, and K. D. Saunders (1990), The origin and characteristics of the Algerian Current, *J. Geophys. Res.*, *95*, 1587–1598, doi:10.1029/JC095iC02p01587.

Benzohra, M., and C. Millot (1995), Characteristics and circulation of the surface and intermediate water masses off Algeria, *Deep Sea Res., Part I*, *42*, 1803–1830, doi:10.1016/0967-0637(95)00043-6.

Dewey, R. K., J. N. Moum, C. A. Paulson, D. R. Caldwell, and S. D. Pierce (1991), Structure and dynamics of a coastal filament, *J. Geophys. Res.*, *96*, 14,885–14,907, doi:10.1029/91JC00944.

Dibarboure, et al. (2008), SSALTO/DUACS user handbook: (M)SLA and (M)ADT near-real time and delayed time products, *Rep. CLS-DOS-NT-06.034*, Collect. Localisation Satell., Ramonville Saint-Agne, France.

Gomis, D., and M. A. Pedder (2005), Errors in dynamical fields inferred from oceangraphic cruise data. Part I. The impact of observations errors and the sampling distribution, *J. Mar. Syst.*, *56*, 317–333, doi:10.1016/j.jmarsys.2005.02.002.

Gomis, D., S. Ruiz, and M. A. Pedder (2001), Diagnostic analysis of the 3D ageostrophic circulation from a multivariate spatial interpolation of CTD and ADCP data, *Deep Sea Res., Part I*, *48*, 269–295, doi:10.1016/S0967-0637(00)00060-1.

Hoskins, B. J., I. Draghici, and H. C. Davies (1978), A new look at the omega-equation, *Q. J. R. Meteorol. Soc.*, *104*, 31–38.

LaCasce, J. H., and A. Mahadevan (2006), Estimating subsurface horizontal and vertical velocities from sea surface temperature, *J. Mar. Res.*, *64*, 695–721, doi:10.1357/002224006779367267.

Le Traon, P. Y., and F. Ogor (1998), ERS-1/2 orbit improvement using T/P: The 2 cm challenge, *J. Geophys. Res.*, *103*, 8045–8057, doi:10.1029/97JC01917.

Lindstrom, S., and D. P. Watts (1994), Vertical motion in the Gulf Stream near 68 degrees, *J. Phys. Oceanogr.*, *24*, 2321–2333, doi:10.1175/1520-0485(1994)024<2321:VMITGS>2.0.CO;2.

McGillicuddy, D. J., et al. (2007), Eddy/wind interactions stimulate extraordinary mid-ocean plankton blooms, *Science*, *316*, 1021–1026, doi:10.1126/science.1136256.

Millot, C. (1985), Some features of the Algerian Current, *J. Geophys. Res.*, *90*, 7169–7176, doi:10.1029/JC090iC04p07169.

Pascual, A. (2003), Different approaches to the circulation in the Balearic Sea: From satellite data to quasigeostrophic dynamics, Ph.D. thesis, 218 pp., Univ. of the Balearic Islands, Mallorca, Spain, 12 June.

Pascual, A., and D. Gomis (2003), Use of surface data to estimate geostrophic transport, *J. Atmos. Oceanic Technol.*, *20*, 912–926, doi:10.1175/1520-0426(2003)020<0912:UOSDTE>2.0.CO;2.

Pascual, A., Y. Faugère, G. Larnicol, and P.-Y. Le Traon (2006), Improved description of the ocean mesoscale variability by combining four satellite altimeters, *Geophys. Res. Lett.*, *33*, L02611, doi:10.1029/2005GL024633.

Pinot, J. M., J. Tintoré, and D.-P. Wang (1996), A study of the omega equation for diagnosing vertical motions at ocean fronts, *J. Mar. Res.*, *54*, 239–259, doi:10.1357/0022240963213358.

Pollard, R. T., and L. A. Regier (1992), Vorticity and vertical circulation at an ocean front, *J. Phys. Oceanogr.*, *22*, 609–625, doi:10.1175/1520-0485(1992)022<0609:VAVCAA>2.0.CO;2.

Rio, M.-H., P. M. Poulain, A. Pascual, E. Mauri, G. Larnicol, and R. Santoleri (2007), A mean dynamic topography of the Mediterranean Sea computed from altimetric data, in-situ measurements and a general circulation model, *J. Mar. Syst.*, *65*, 484–508, doi:10.1016/j.jmarsys.2005.02.006.

Rodríguez, J., J. Tintoré, J. T. Allen, J. Blanco, D. Gomis, A. Reul, J. Ruiz, V. Rodríguez, F. Echevarría, and F. Jiménez-Gómez (2001), The role of mesoscale vertical motion in controlling the size structure of phytoplankton in the ocean, *Nature*, *410*, 360–363, doi:10.1038/35066560.

Ruiz, S., A. Pascual, B. Garau, Y. Faugere, A. Alvarez, and J. Tintoré (2009), Mesoscale dynamics of the Balearic Front, integrating glider, ship and satellite data, *J. Mar. Syst*, doi:10.1016/j.jmarsys.2009.01.007, in press.

Shearman, R. K., J. A. Barth, and P. M. Kosro (1999), Diagnosis of the three-dimensional circulation associated with mesoscale motion in the California Current, *J. Phys. Oceanogr.*, *29*, 651–670, doi:10.1175/1520-0485(1999)029<0651:DOTTDC>2.0.CO;2.

Siedler, G., J. Church, and J. Gould (2001), *Ocean Circulation and Climate*, *Int. Geophys. Ser*, vol. 77, edited by R. Dmowska, J. R. Holton, and H. T. Rossby, Academic, London.

Strass, V. H. (1994), Mesoscale instability and upwelling: Part 2. Testing the diagnostics of vertical motion with a three-dimensional ocean front model, *J. Phys. Oceanogr.*, *24*, 1759–1767, doi:10.1175/1520-0485(1994)024<1759:MIAUPT>2.0.CO;2.

Tintoré, J., P. E. LaViolette, I. Blade, and A. Cruzado (1988), A study of an intense density front in the eastern Alboran Sea: The Almeria–Oran front, *J. Phys. Oceanogr.*, *18*, 1384–1397, doi:10.1175/1520-0485(1988)018<1384:ASOAID>2.0.CO;2.

Tintoré, J., D. Gomis, S. Alonso, and G. Parrilla (1991), Mesoscale dynamics and vertical motion in the Alboran Sea, *J. Phys. Oceanogr.*, *21*, 811–823, doi:10.1175/1520-0485(1991)021<0811:MDAVMI>2.0.CO;2.

B. Garau, A. Pascual, S. Ruiz, and J. Tintoré, Instituto Mediterraneo de Estudios Avanzados, IMEDEA (CSIC-UIB), C/Miquel Marquès, 21, E-07190 Esporles, Spain. (simon.ruiz@uib.es)

I. Pujol, CLS, 8-10 Rue Hermes, F-31520 Ramonville Saint-Agne CEDEX, France.